Study of Frequency Independent Antennas Final Report

1 May 1960–30 June 1961

DA 36-039 SC-84923

October 15, 1961

ELECTRONICS RESEARCH LABORATORY

UNIVERSITY OF CALIFORNIA
BERKELEY, CALIFORNIA

Electronics Research Laboratory
University of California
Berkeley, California

STUDY OF FREQUENCY INDEPENDENT ANTENNAS

Final Report

1 May 1960 - 30 June 1961

by

V. H. Rumsey
W. J. Welch
G. Borgiotti
M. J. Gans
R. Sussman

Object: To develop frequency independent antennas which have any prescribed radiation pattern, polarization and impedance.

Signal Corps Contract DA 36-039 SC-84923
Department of the Army Task No. 3A99-23-001-01

U. S. Army Signal Research and Development Laboratory
Fort Monmouth, New Jersey

TABLE OF CONTENTS

PURPOSE

The purpose of this contract is to investigate frequency-independent antennas from the point of view of designing the antennas for any radiation pattern and polarization.

ABSTRACT

During the past year solutions of Maxwell's equations have been discovered which explain the theory of frequency independent antennas. The effect of curvature on the current distribution is strikingly demonstrated but the most remarkable feature is the incoming current wave at large distances, when the angular phase velocity of the excitation is in the direction of decreasing radius along an equiangular spiral. Solutions for periodic antennas have also been obtained and extensive computations are being made.

PREVIOUS REPORTS

The work during the past year has been principally centered around the theoretical solution which was obtained a little over a year ago. In the first place this solution was found to give a standing wave for the current distribution at large distances from the source, a result which caused some difficulty because it was contrary to measurements. After considerable effort, this difficulty was overcome and a new version of the theory, which has so far survived a number of careful checks, now gives an outgoing traveling wave for the current distribution, in the case where the antenna is excited so that the angular phase velocity is in the direction of increasing radius along the spiral. However, when the excitation corresponds to an angular phase velocity in the opposite direction, we obtain a current distribution at large distances consisting of an inward traveling wave, which is a most remarkable result.

The current distribution has been obtained directly from the integral transform by using a digital computer and, alternatively, explicit formulas have been worked out for large and small values of the distance from the center. We have been fortunate in being able to obtain the first three terms of the asymptotic formula for the current at large distances. This shows most clearly how the curvature of the spiral causes the current to be attenuated and is thus the first known solution of Maxwell's equations for a frequency independent antenna. The backward traveling wave mentioned in the previous paragraph is, of course, a point of most intense interest. It is being pursued not only by the group at Berkeley, but also by the group at Illinois, who have noticed some very unusual effects when the spiral is excited in what might be called the "unnatural way."

Several other theoretical approaches are under way. One is the new way of solving Maxwell's equations based on decomposing the general solution into what may be roughly called the right and left handed circularly polarized parts. The results, when applied to plane waves, connect nicely with the asymptotic solution mentioned in the previous paragraph and the current work on this subject shows

promise of giving a much clearer understanding of frequency independent antennas. The problem of an antenna consisting of sinusoidal wires, with uniform period, has also been solved and extensive calculations of the results are just now being completed. Although incomplete, this work shows most of the features which have been observed in connection with periodic types of frequency independent antennas and should give a detailed picture of how these antennas work. A considerable amount of work has also been done on conical antennas but so far this has not resulted in useable solutions. The prospects for obtaining a solution look quite promising.

The current experimental work consists of the following investigations: the phase and amplitude distributions of the radiation field for multielement spiral antennas, especially two, four, and six element versions, the checking of the theoretical solution on a model consisting of ten or twenty spiral wires, the development of microwave transducers which can be designed to give angular phase velocities corresponding to complete rotations of 2π, 4π, 6π, etc., the properties of multielement spiral antennas as transducers in the cross section of a circular waveguide, and the investigation of propagation over a sheet of sinusoidal wires.

Since much of this work has been described in previous reports or will be described in reports which are now in process of publication, we will first quote the abstracts of these reports and then provide detailed information on the work which they do not cover:

Title: "A Complete Orthogonal Set of Solutions for Maxwell's Equations with Applications to Anisotropic Sheets."
Author: V. H. Rumsey
Issue: No. 287
Date: June 15, 1960

SUMMARY

A general solution of Maxwell's equations for a single frequency can be expressed as the combination of two types of solution each of which is characterized by an electric vector which is equal to the magnetic vector times the intrinsic impedance of free space but a quarter cycle out of phase. These two types are mathematically orthogonal

and each can be conveniently expressed by means of a single scalar. The method leads to simple solutions for propagation along anisotropic sheets which are perfectly conducting in one tangential direction and perfectly transparent in the orthogonal tangential direction.

Title: "A New Way of Solving Maxwell's Equations."
Author: V. H. Rumsey
Issue: No. 335
Date: December 19, 1960

SUMMARY

This is a radical revision of report No. 287 in which a number of physical applications are worked out in detail.

Title: "A Solution to the Equiangular Spiral Antenna Problem."
Author: Bernard Ru-Shao Cheo
Issue: No. 324
Date: November 1, 1960

SUMMARY

A theoretical investigation was made on an antenna consisting of an infinite number of coplanar equiangular spiral wires. A solution was obtained in a form capable of giving most of the features of interest in this antenna. In most respects, the results obtained are in good agreement with experimental observations made on practical structures of this same general shape.

By expressing the solutions to Maxwell's equations in terms of the modes for which the electric and magnetic field phasors are related by $\vec{E} = \pm j\sqrt{\mu/e}\,\vec{H}$, it was possible to reduce the problem to that of finding a scalar wave function, from which all the field components may be derived. All the necessary boundary conditions can be included in a partial differential equation which the wave function must satisfy on the surface of the antenna. Through the application of the Hankel transform on the boundary condition, the exact wave function was found. Using this wave function, any field component or the current distribution on the structure can be expressed in terms of a known integral. Methods of asymptotic integration were used to obtain the behavior of the solution both near to and far from the point of excitation. Near

the input the current and voltage are finite and constant along the wires. A far zone evaluation shows that the current density on the structure is an outgoing wave with amplitude diminishing as $1/r^2$. A digital computer evaluation has shown that the current distribution begins as a slow backward wave then gradually turns into a fast backward wave and then into a fast forward wave which slows down to the velocity of light. For the particular mode of excitation corresponding to that of a two arm antenna, the radiation is broadside with a single lobe at each side of the antenna. The minimum beamwidth is approximately 70 degrees corresponding to tightly wound spirals.

Title: "A Solution to the Frequency-Independent Antenna Problem."
Authors: B. Cheo, V.H. Rumsey, and W.J. Welch
Issue: No. 372
Date: June 14, 1961

SUMMARY

A solution of Maxwell's equations is obtained for an antenna consisting of an infinite number of equally spaced wires in the form of coplanar equiangular spirals. Radiation amplitude patterns obtained from this solution agree closely with measurements on two-element spiral antennas. The phase pattern shows the approximate validity of a phase center at a distance behind the antenna which decreases with the tightness of the spiral. The current distribution clearly shows increased attenuation with increase in the tightness of the spiral thus showing how the frequency-independent mode depends on the curvature. A remarkable feature of the solution is that the current consists of an inward traveling wave at infinity when the antenna is excited in that sense which produces an outward wave at the center.

Title: "Propagation over a Sheet of Sinusoidal Waves with Application to Frequency Independent Antennas."
Authors: G. Borgiotti and V.H. Rumsey
Issue: To be published

SUMMARY

An exact solution of Maxwell's equations is obtained for a sheet of sinusoidal waves infinitely close together thus forming a two sided

anisotropic surface. The solution shows that the structure acts as a waveguide at frequencies below a certain critical value and as an antenna at higher frequencies. The characteristics of the structure as a waveguide and antenna are plotted on a Brillouion diagram, which clearly shows how the "active" region in logarithmically periodic antennas first arises in connection with a backward fast wave.

Title: "Polarization Properties of Plane Equiangular Spiral Antennas"
Author: J. Siambis
Issue: To be published

SUMMARY

The polarization of the far field of the plane equiangular spiral antenna was investigated at 3000 MC with respect to the tightness of the spiral. The measurements showed that the polarization is circular and does not vary appreciably with the tightness of the spiral for angles inside the half-power beamwidth of the antenna. For angles beyond the half-power beamwidth the axial ratio of the polarization ellipse varies appreciably with the tightness of the spiral and there exists an optimum tightness for which the polarization remains circular to an angle over 80 degrees off the main axis of the antenna. The polarization pattern has been compared with the theoretical patterns for two halfwave dipoles in phase quadrature and a circular loop of one wavelength circumference the phase of the current being equal to the azimuthal angle. The experimental results are closely approximated by the latter.

Title: "The Equiangular Plane Spiral Antenna"
Author: R. Sussman
Issue: To be published

The "Equiangular Plane Spiral Antenna" belongs to the class of "Frequency Independent Antennas," a class which has recently drawn much attention.

In view of the fact that there has not yet been found a solution for the electromagnetic field of the "Equiangular Plane Spiral Antenna" with a finite number of arms, its field is investigated here mainly experimentally. In particular, the pattern, the phase variation, and the polarization of the field of spiral antennas with a small number of arms,

as generated by various methods of excitation, are examined.

In order to achieve this, a method of decomposing any complicated feeding arrangement into a set of "basic" feedings has been developed. This method is not restricted to spiral antennas, but can be applied also to any equally spaced plane antenna with any number of arms.

Next, measurements on 2-, 4-, and 6-arm spiral antennas have been performed. The results of the measurements show that the solution recently found for the limiting case of a spiral antenna which has an infinite number of arms, can serve as a good approximation to antennas with a small number of arms. Some correction terms, which depend on the number of arms, are introduced into the solution of the "infinite" arm antenna, so as to get a still better approximation.

The combination of the method of decomposition into basic feedings with the experimental results leads to an approximate expression for the field of a spiral antenna, with any number of arms and any feeding arrangement.

Title: "Phase Distributions of Spiral Antennas"
Author: N. Barbano
Issue: No. 266
Date: January 8, 1960

The phase distributions of four types of equiangular spiral antennas were investigated at 3,000 mc. The measurements show that an apparent phase center exists for each antenna. It was found to lie directly behind the feed point. With different orientations of each spiral antenna the distance of the phase center from the feed point varied.

An additional experiment was performed to determine if the finite size of the equiangular spiral antennas had any effect on the location of the phase center. It was discovered that the location was sensitive to the size of the antenna, i. e., the location of the phase center changed with the diameter.

The apparent phase centers were located by first determining several equiphase fronts of the spiral antennas and then finding the location of the phase center from the results. The equiphase fronts

were determined by using an Adcock direction finding antenna. Since only one Adcock antenna was used, only one direction of linear polarization was measured.

Title: "A General Way of Representing the Electromagnetic Field With Application to Anisotropic Surfaces"
Author: G. Borgiotti
Issue: To be published

After a brief outline of the method of Fourier transform in electromagnetic theory, it is shown on the basis of some general properties of matrix calculus that any arbitrary electromagnetic field can be expressed through two scalar functions in an infinite number of ways. These functions, f_1 and f_2, are interpreted as coordinates of the electric field in a bidimensional space referred to two linearly independent vectors. The field can be alternatively expressed through two different scalar functions, g_1 and g_2, which are the coordinates of the magnetic field in the same vector space. The functions g_1 and g_2 are linearly dependent upon f_1 and f_2. Therefore in vector notation

$$\vec{f} = [M]\,\vec{g}$$

The determinant of [M] is equal to the square of the intrinsic impedance of the medium . It is shown that if orthogonal vectors are chosen for the basis, a type of representation is obtained which is coincident with the classical decomposition of a field into TE and TM parts. The TE and TM solution is therefore only a particular case of a more general way of representing the electromagnetic field. An alternative representation in terms of the eigenvectors of [M] leads to a decomposition of the general solution into two components characterized by $\mathcal{E} = \pm j\mathcal{H}$, $\mathcal{E}$ and $\mathcal{H}$ being the Fourier transforms of the electric and magnetic fields, and $\pm j\eta$ the eigenvalues of [M] .

Two applications of the general method are described. The first one is concerned with the problem of back-scattering and transmission

of a plane monochromatic wave incident on an anisotropic plane sheet of straight wires infinitely thin and infinitely close together. The general solution for an arbitrary direction of incidence and an arbitrary polarization is found, using a vector basis corresponding to the decomposition of the electric field into two components orthogonal to x and y axes (z = 0 being the equation of the plane and x being the direction of the wires). An explicit expression is found for the relationships between the horizontal and vertical components of the incident field, and the corresponding components of the scattered and transmitted fields.

The second example concerns a similar anisotropic surface with all the wires parallel to the same sinusoid. Using the eigenvectors of [M], a surface wave type of solution is found in the form of a series. It is shown that the coefficients of space harmonics converge rapidly for harmonics of positive and negative order, respectively to $J_n(\gamma_1)$ and $J_{|M|}(-\gamma_2)$, γ_1 and γ_2 being two constants proportional to the frequency. These coefficients are related by a recurrence formula that for high values of $|n|$ tends to the well known relationship among Bessel functions of the same argument

$$J_{n-1}(z) + J_{n+1}(z) = \frac{2n}{z} J_n(z)$$

Using this property, a formula is derived for the numerical computation of the principal propagation constant.

WORK NOT COVERED IN THE PREVIOUS REPORTS

1. Excitation of the planar multiarm equiangular spiral antenna at "X" Band.

There are several reasons for exciting the planar multiarm antenna at "X" band. First, operation of antennas at "X" band simplifies the procedure for pattern measurements. The other advantages arise from the type of excitation procedure enforced by the size of the "X" band antenna. Since the excitation must be confined to a region which is less than about one-eighth wavelength in diameter, it is extremely difficult to construct a coaxial line which will lay on top of and wind in with an arm of the spiral antenna as is the usual method of excitation for spiral antennas at "S" band and lower frequencies. Therefore, at "X" band the only practical method of excitation is to feed the antenna at its center by menas of a waveguide normal to the plane of the antenna. Since this method does not require a coaxial line for each pair of arms on the antenna, it is possible to construct the antenna with many arms and thereby allow experimental antennas to approximate the ideal antenna, which has an infinite number of arms. By making a close approximation to the ideal antenna, it may be possible to determine the reason for the disagreement between the theoretically predicted field of the ideal antenna and the measured field obtained from the spiral with only several arms. (For instance, the ideal antenna is supposed to give the same pattern independent of the sense of polarization of the input, whereas the spiral antenna with several arms will radiate only one sense of polarization.) This method also allows reversing the sense of polarization of the input without reconnecting leads to the antenna arms.

There is a disadvantage to exciting the antenna by a waveguide normal to the antenna when the excitation is $e^{\mp j\phi}$ (see figure 1.) because the waveguide is at the maximum of the field pattern of the antenna and does represent a major disturbance to the frequency-independent mode of the antenna. However, for $e^{\mp jn\phi}$ excitation, where n is greater than

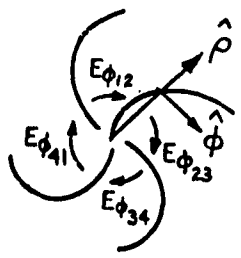

$\pm e^{jn\phi}$ excitation means that the voltage applied at a certain instant to each arm of the spiral varies as $\sin(n\phi_i)$, where ϕ_i is the coordinate of the particular arm with respect to a reference axis that is rotating in the $\pm\phi$ direction at the radio frequency.

Figure 1. Excitation Coordinates

1, the antenna pattern has a null in the direction normal to its center and thus the waveguide should not disturb the field. Thus, this method of excitation should have practical applications.

a. $\pm e^{j\phi}$ Excitation

Since, as shown in figure 1, the $\pm e^{j\phi}$ excitation would require a mode in a circular cylindrical feed waveguide whose $\hat{\phi}$ component varied as $\sin\phi$, while the reference axis for ϕ rotated with time, the obvious solution for this problem was to provide a rotating TE_{11} mode by using some form of quarter wave plate. The first tests were performed with a capacitance stub type of quarter wave plate which was already available in the laboratory. However, this quarter wave section was found to be too frequency sensitive to be practical. A dielectric quarter wave plate of the type shown in figure 2 was then constructed and was found to give an axial ratio of less than 1.2:1 over the range of frequencies from 9400 - 9600 mc. Lucite was used primarily for ease

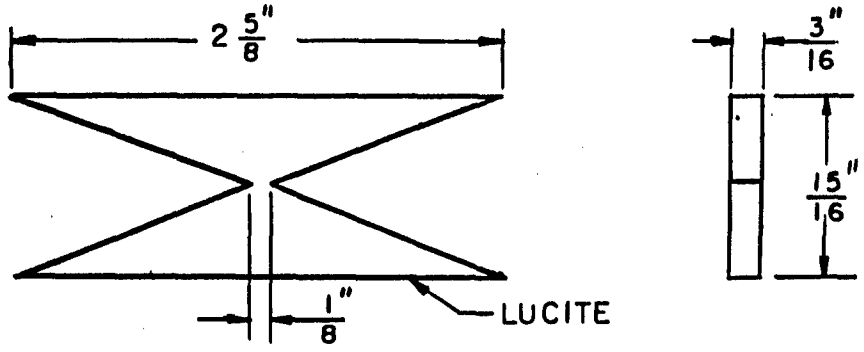

Figure 2. Dielectric Quarter Wave Plate

of machining, and, although other materials such as polyethelene introduce less loss, the loss introduced by the lucite was not noticeable.

The TE_{11} mode can be broken down into two orthogonal TE_{11} mode components. The way in which the dielectric quarter wave plate works is by shifting the phase of the component, whose maximum concentration lines up with the quarter wave plate, one quarter wave length with respect to the other component. Thus, since the components are displaced azimuthally by 90° and one component lags the other by 90° in time, the total field will rotate towards the left or right depending on which component lags. Therefore, the sense of rotation may be reversed by merely turning the quarter wave plate 90° in the waveguide.

The method by which the quarter wave plate was tested was to measure the radiation from the circular guide, with the quarter wave plate inside, by means of two helical antennas wound in opposite sense. The helical antennas were designed so that the size and spacing of the turns would cause each of the two helical antennas to radiate right and left handed circular polarization, respectively, on their axes. The helical antennas were checked by rotating a receiving horn on the axis of the far field pattern of the helix, and these measurements indicated that the axial ratio of the far field of the helical antennas was 1.2:1 at 9500 mc. The construction of the helical antenna is shown in figure 3.

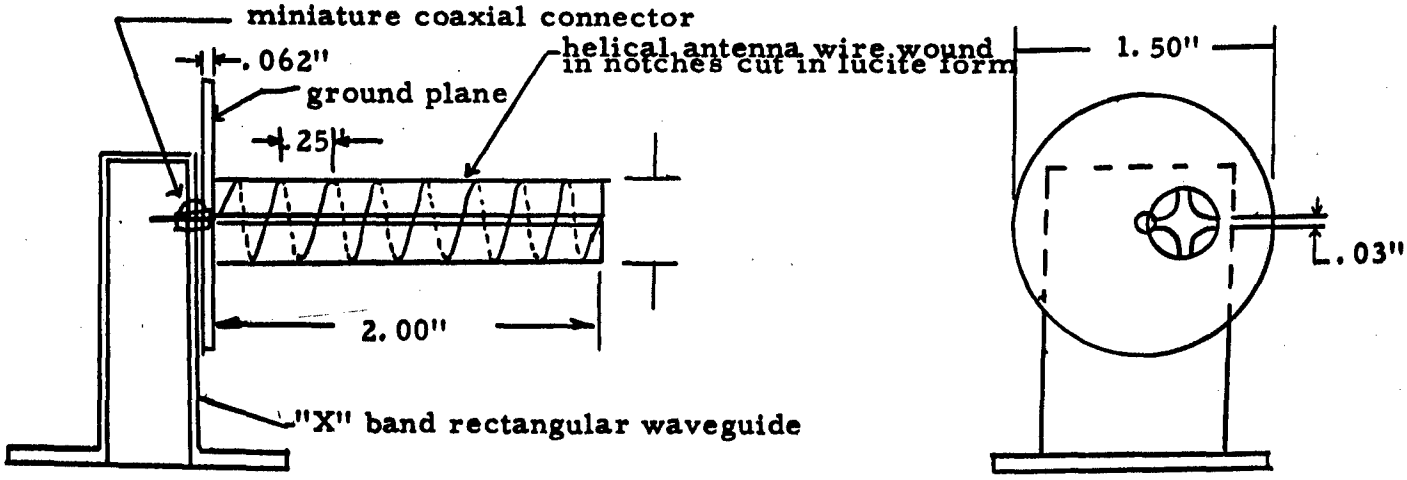

Figure 3. Helical Antenna

Now, the way in which the helical antennas were used to construct the quarter wave plate was to receive the radiation from the circular guide, in which the quarter wave plate was placed, by both senses of helical antennas and then measure the ratio of the signals received by each of these helical antennas on a ratio-meter. Thus, a continuous reading was given as the quarter wave plate was adjusted or the signal generator frequency varied. When a ratio of more than 20 db was registered on the ratio meter, finer adjustments were then made by measuring the axial ratio of the field radiated from the circular guide by means of rotating a rectuangular horn type receiving antenna.

After obtaining the rotating TE_{11} mode as described above, two methods of exciting the spiral antenna were attempted. The first method was to make a gradual transition from the hollow circular waveguide to a coaxial guide of the same outer dimension to give a rotating TE_{11} mode now in a coaxial guide. A spiral antenna was then constructed by shaping a block of polyfoam to fit tightly over the flange of the waveguide and then 16 equiangular spirals were drawn with a machine, previously constructed, on a circular sheet of polystyrene. Thin wires were placed along the lines and glued to this sheet. The sheet was then glued to the polyfoam block, placing the antenna 1/4 inch in front of the waveguide flange. The center conductor of the coaxial guide was then brought through the polyfoam block and polystyrene sheet and connected to all the wire arms of the antenna. (See figure 4.)

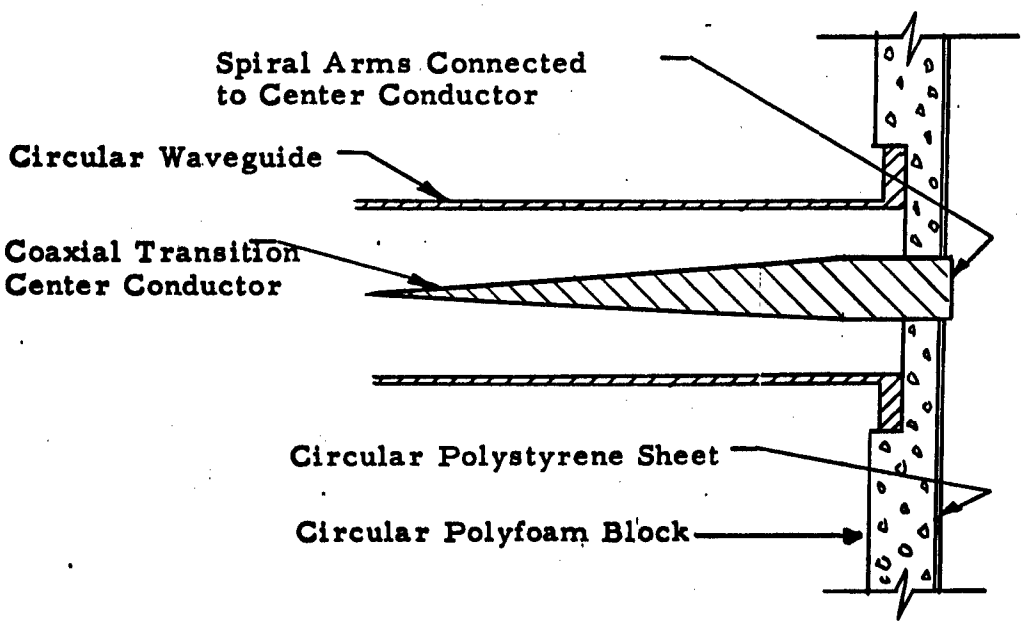

Figure 4. Spiral Antenna Type 1.

Radiation patterns were then measured for this antenna. The patterns were not the same as those predicted by the ideal antenna theoretical solution. An attempt was then made to separate out that part of the pattern which might indicate the presence of the frequency-independent mode. Two methods were used: First, an antenna similar to that shown in figure 4, but using radial wires was used. It was believed that this would point up the effect of the spiral wires; however, the results were not conclusive. The other method was to reverse the polarization of the feed which, by measurements at "S" band, had been found to give a null on the axis of the pattern for the frequency-independent mode. Again the results were inconclusive. An example of the patterns recorded in this way is shown in figure 5. It was decided, from the shape of the patterns, that the size of the feed waveguide was too large for two reasons: First the direct radiation from the guide was much stronger than any radiation from the spiral wires and, also, the spiral antenna should not be excited over an area which includes the active radiating region of the antenna, if it is to coincide with the assumptions used in obtaining the theoretical solution to the ideal antenna. To minimize the aperture of the feed waveguide, a new waveguide was constructed which contained a high permittivity dielectric so that it could be made much smaller without cutting off the rotating TE_{11} mode. At the junction with the antenna, the guide is less than one eighth wavelength in diameter, so that interference with the proper antenna current distribution was minimized. The criterion for the allowable diameter of the excitation apparatus is based on the phase plot found from the solution of the ideal equiangular planar spiral antenna, as shown in figure 6. Since the greatest amount of radiation occurs in the region where the current has the greatest phase velocity, and the least radiation occurs in the region where the current has the slowest phase velocity. It is possible to disturb the current distribution within a radius of $\lambda/16$ of the center of the antenna and yet affect the radiation of the antenna very little.

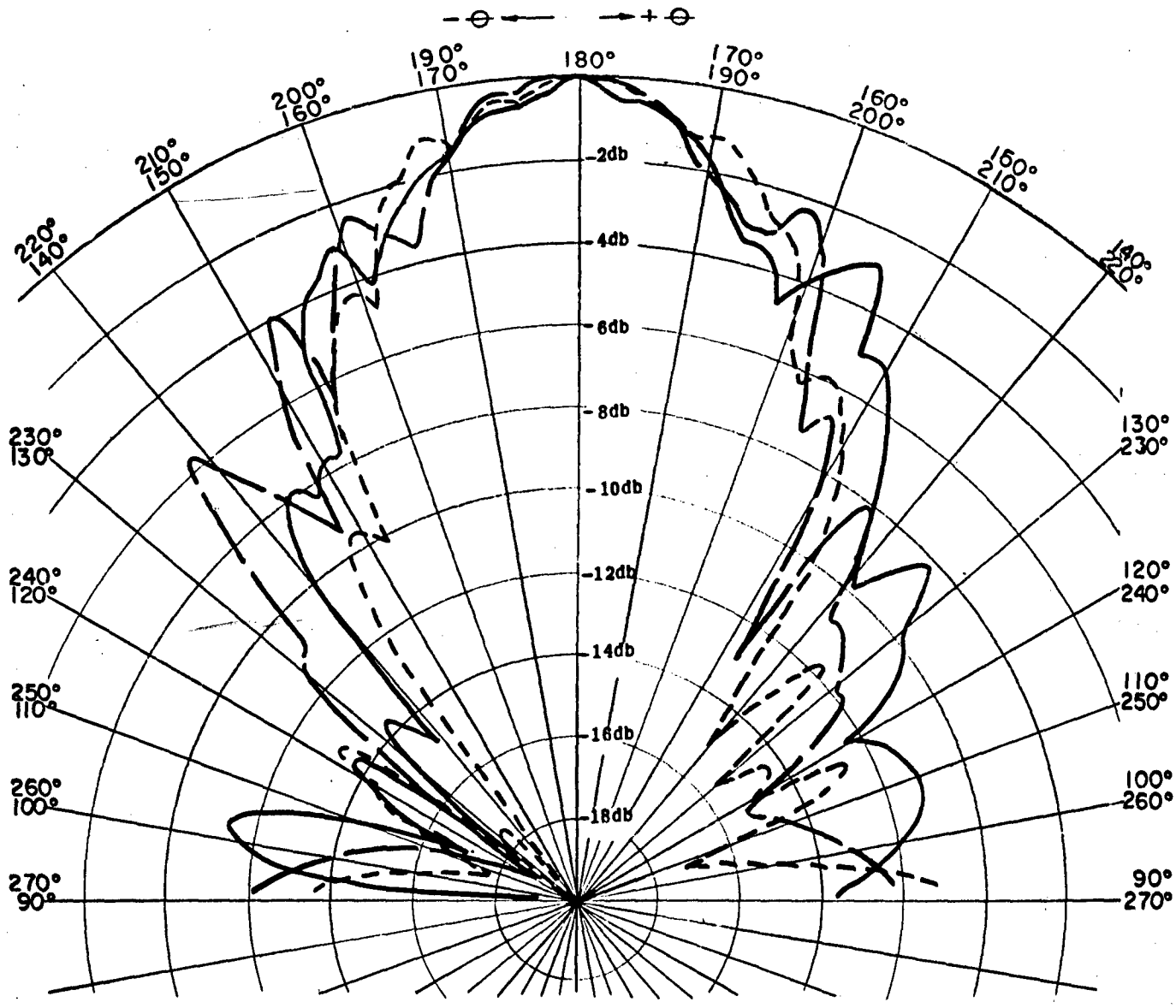

——— Spiral Antenna, L. H. Polarization

— — — Spiral Antenna, R. H. Polarization

— — — — Radial Antenna, L. H. Polarization

Polar Plots of Data Recorded from Antenna Type 1.

Figure 5. Patterns of Antenna Type 1

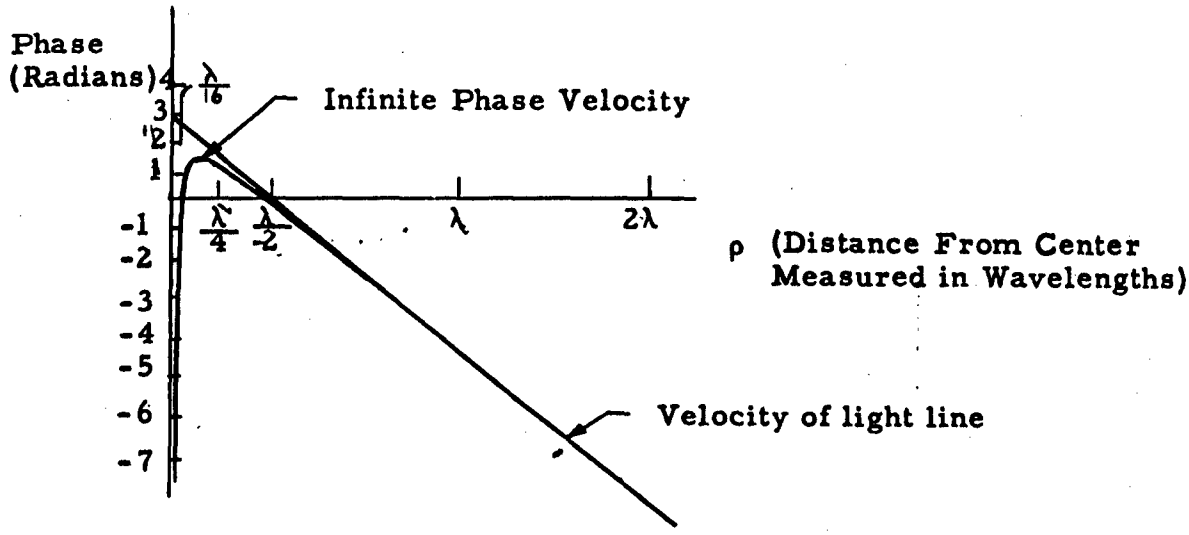

Figure 6. Computed Phase of Current on Ideal Antenna[1]

Also, a new spiral antenna was constructed to be used with this feed waveguide. A thin sheet of teflon was prepared with six equiangular spiral arms photo-engraved on one side. The width of the arms increased as they became further from the center, so that the antenna was a self-complementary antenna. Again the feed waveguide contained a hollow to coaxial transition and the center of the coaxial guide was brought through the teflon sheet and soldered to all the spiral arms. Besides allowing the guide to be made smaller without cutting of the TE_{11} mode, the coaxial center was supposed to provide better coupling of the guide to the antenna. The tapered feed waveguide and photo-engraved antenna are shown in figure 7.

The patterns measured from this antenna did not give definite indication of the presence of the frequency independent mode. The direct radiation from the feed guide was greatly reduced, however, because the received signal with the antenna connected to the guide was 10 db above that received without the antenna connected to the guide. To minimize any effects due to the feed guide disturbing the pattern because it is located in the maximum of the backward pattern of the spiral

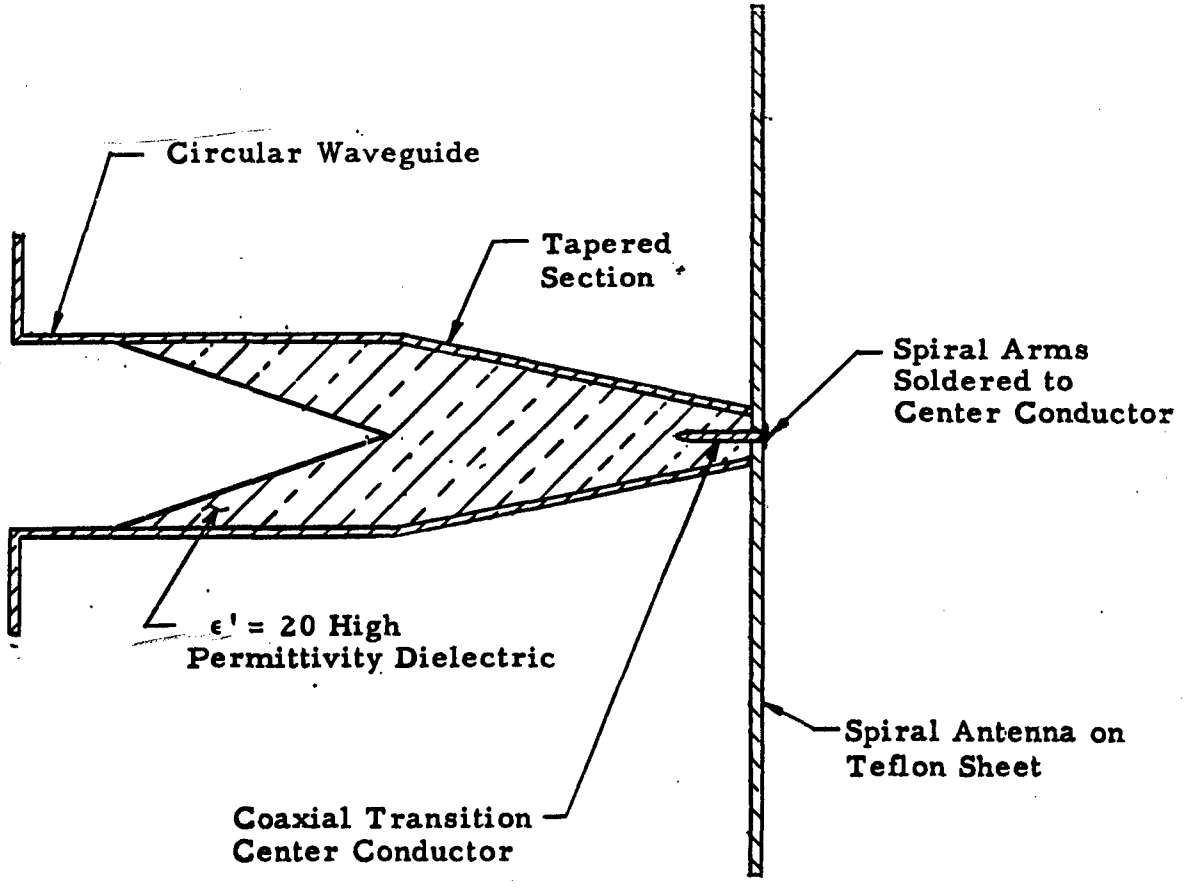

Figure 7. Spiral Antenna Type 2

antenna, a 1/8 inch thick ground plane was constructed two feet on a side with a circular hole in the center where the spiral antenna was located. However, the patterns measured with the ground plane still did not definitely indicate the presence of the frequency-independent mode. The main methods of checking for the presence of the frequency-independent mode were: a) the shape of the pattern, (the frequency-independent mode always has a null in its pattern in the plane of the spiral); b) the frequency-independent mode should give a high ratio, at all points of its pattern, between the received voltage of the right hand helical antenna and the received voltage of the left hand helical antenna. Also, this ratio should reverse when going from the pattern in front of the spiral antenna to the pattern in back of the spiral antenna. An example of some of the patterns obtained by these measurements is shown in figure 8. In a further attempt to minimize reflections from the feed guide, absorbing material was packed around it, behind

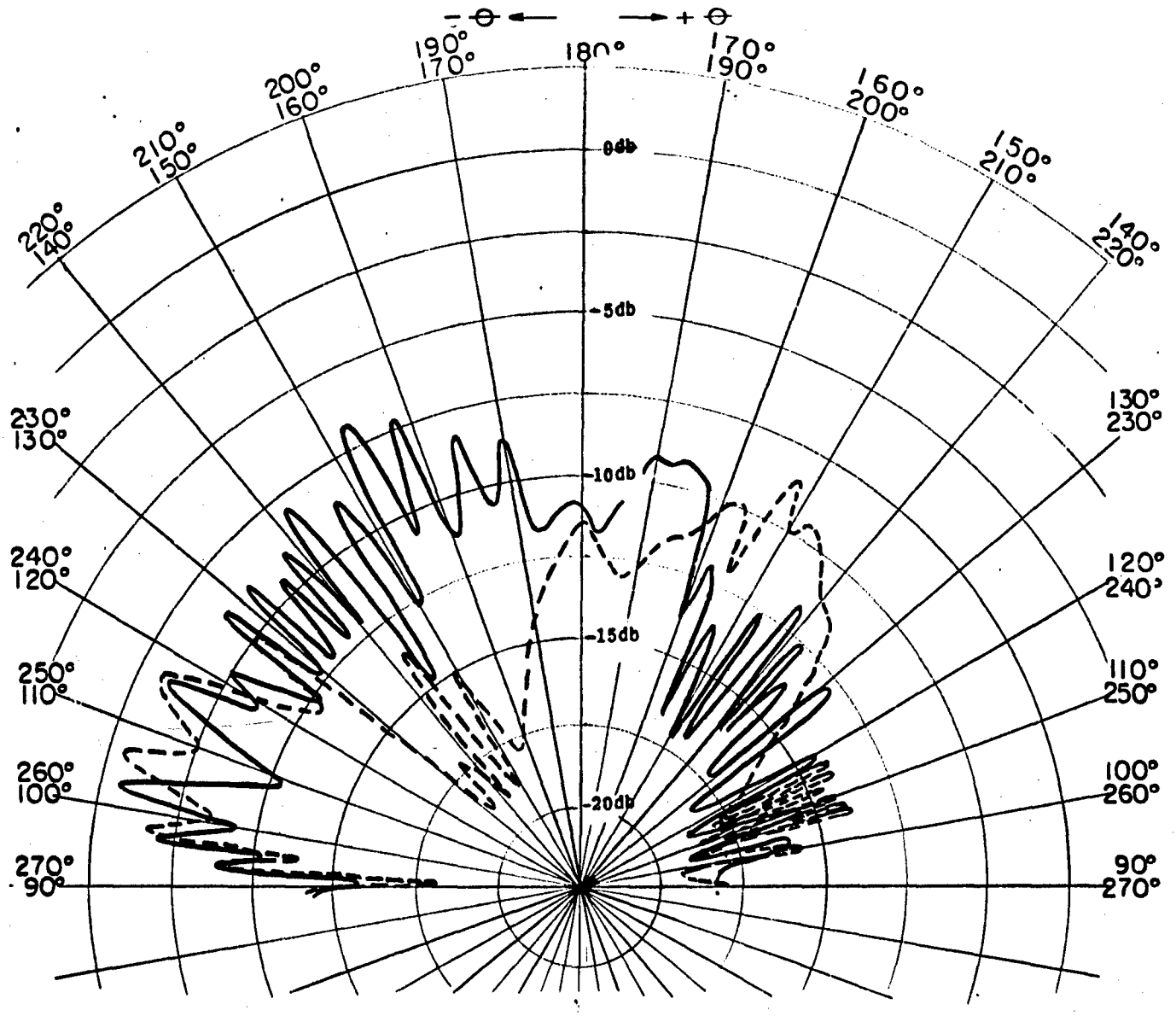

——— Feed L. H. Polarized with Ground Plane and Spiral Antenna and Helix #1 (Right Hand Helix)

– – – – Feed L. H. Polarized with Ground Plane and Spiral Antenna and Helix #2 (Left Hand Helix)

Figure 8. Patterns of Spiral Antenna Type 2.

the spiral antenna and ground plane.

The most plausible reason for the difficulty in launching the frequency-independent mode on the multiarm planar spiral antenna with a tapered circular waveguide at the center is that the guide is not effectively coupled to the antenna. Up to now, the coupling of the guide to the antenna was accomplished by connecting the center conductor of the coaxial guide to all the arms of the antenna, while the outer conductor remained unconnected. An alternative method would be to excite an input guide whose outer conductor is divided into as many equal longitudinal sections as there are arms on the spiral antenna. The previously mentioned dielectric loaded tapered circular waveguide would feed the sectionalized waveguide, which will in turn set up a TEM version of the rotating TE_{11} mode. All TE and TM modes would be cut off because of the small size of the guide. Thus when each arm of the spiral antenna is connected to a corresponding section of the sectionalized circular waveguide, the excitation would be predominantly the $e^{\pm j\phi}$ mode.

In order to provide a rotating mode in a waveguide over a wider frequency range than the dielectric quarter wave plate does, a theoretical investigation of the helix enclosed in a waveguide was carried on. Because the helical antenna provides circularly polarized radiation on its axis over quite a broad frequency range, it is suggested that the helix in an enclosed waveguide might be a good method of providing a rotating mode. The method of theoretically checking whether this is so or not, was to derive the dispersion relationship by matching the boundary conditions and then drawing the ω-β diagram from the dispersion relationship. It was then hoped that the ω-β diagram would show that it was possible to design the helix so that all modes except the desired mode would be cut off at the range of frequencies of interest. As a simpler approach to the problem, a sheath helix in a circular cylindrical guide was first assumed and the following dispersion relationship was obtained:

$$\frac{-\omega^2 \mu_0 \epsilon_0 a^2}{\left[\frac{\beta n}{\tau} - \tau a \tan x\right]^2} = \left[\frac{J_n(\tau a)}{J_n'(\tau a)}\right]\left[\frac{J_n'(\tau b)}{J_n(\tau b)}\right]\left[\frac{J_n(\tau a)N_n(\tau b) - J_n(\tau b)N_n(\tau a)}{J_n'(\tau a)N_n'(\tau b) - J_n'(\tau b)N_n'(\tau a)}\right] \quad (1)$$

where: n = number of field variations with ϕ

a = radius of the helix

b = radius of the enclosing waveguide

ψ = lead angle of the helix

τ = propagation constant along the guide

and $\tau^2 + \beta^2 = \omega^2 \mu_0 \epsilon_0$

However, equation (1) could only be plotted accurately on an ω-β diagram with the help of a computer. As an alternative method of plotting the ω-β diagram, one can draw approximate curves by assuming certain quantities negligible; then these curves may be joined together, in regions where the approximations are not valid, by the coupling of modes methods. In order to know how to join these curves it was expected that the solution of the planar helix would be simple enough to solve exactly and thus indicate the method of joining the curves of the circular helix. The planar helix consists of two infinite parallel anisotropic planes, one conducting in the $y + z \tan \psi$ direction and the other in the $-\hat{y} + \hat{z} \tan\psi$ direction, both placed between to infinite parallel metallic planes. (See figure 9.)

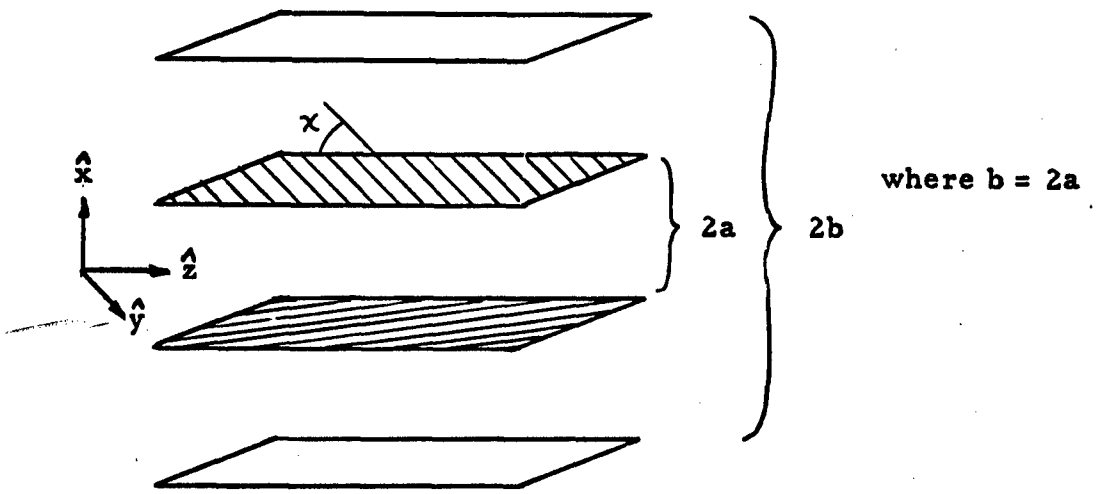

Figure 9. Planar Helix

The dispersion relationship for the n = 0 case was indeed simple, (no variation in field with y).

$$\frac{(\tau a)^2}{1 + \tanh^2(\tau a)} = 12.5\, \omega^2 \mu_0 \epsilon_0 a^2 \tag{2}$$

where: $\tan \psi = 1/5$ (assumed)

β = propagation constant in $\hat{z}$ direction

and: $\tau^2 + \beta^2 = \omega^2 \mu_0 \epsilon_0$

This relationship was found to give an ω-β diagram very close to that of the n = 0 mode of a circular sheath helix in free space. However, the dispersion relationship for n > 0 was found to be too complicated to be any help in plotting equation (1).

$$\left[\coth(\tau a) - 1 + \frac{e^{\tau a}}{\sinh(\tau a)}\right]\left[n^2 - \tau^2 - \beta n \cot\psi\right] +$$

$$\left[\tanh(\tau a) - 1 + \frac{e^{\tau a}}{\sinh(\tau a)}\right] \frac{\omega^2 \mu_0 \epsilon_0 \tau^2 \cot\psi}{(\tau^2 - n^2)\tan\psi + \beta_n} = 0 \tag{3}$$

From looking at the equations, it does not seem very probable that there will be any frequency at which all modes except the desired mode is cutoff; however, it is possible to insert mode filters to eliminate certain modes. For instance, if it were desired to suppress the n = 0 mode, a lossy rod could be placed in the center of the guide where the n = 0 mode has a maximum concentration of field while the n > 0 modes have a null at that position. If one particular n is desired, then a lossy tube could be placed at a radius where this mode has a zero and thus all other modes would be suppressed. However, these methods are inherently frequency sensitive. The helix in a waveguide does, however, have some points which recommend that it be further investigated. First, it may be possible, by using a multifilar helix to excite the desired $\pm e^{jn\phi}$ voltage variation between the wires of the helix. The

multifilar helix could then be tapered down and traightened out into a small multiconductor polyphase cable carrying a rotating TEM mode. Each of the wires of this cable could then in turn be connected to a corresponding arm of the spiral antenna, thus providing possibly a good coupling from the feed to the antenna. Another reason for further investigating the helix in a waveguide is to provide comparison between the effect of doupling of modes when radiation is is not allowed, as for the helix in free space. Much attention is being paid to the explanation of radiation from periodic structures by the coupling of certain modes and perhaps the above investigation may prove helpful.

b. $\underline{e^{\pm jn\phi}}$ Excitation

As mentioned before, the $e^{\pm jn\phi}$ excitation ($n > 1$) is important because it will allow us to bring in the feed waveguide without disturbing the field. Also, the theoretical pattern effects are interesting to note as we vary n, and it is desireable to verify these results experimentally. It has already been pointed out that the helix in a waveguide might be a possible transducer to provide $e^{\pm jn\phi}$ excitation; however, a much simpler approach is the extension of the dielectric quarter wave plate to the higher order modes. For instance if a TE_{21} mode, which has a $\sin(2\phi)$ field variation, is broken down into its two orthogonal components and a dielectric quarter wave plate is placed in line with the maximum concentration of one of the components, then we would expect to get a rotating TE_{21} mode just as the dielectric quarter wave plate gave us a rotating TE_{11} mode previously. In order to test this hypothesis, a mode transducer was built to provide a TE_{21} mode in a circular waveguide. This transducer is shown in figure 10.

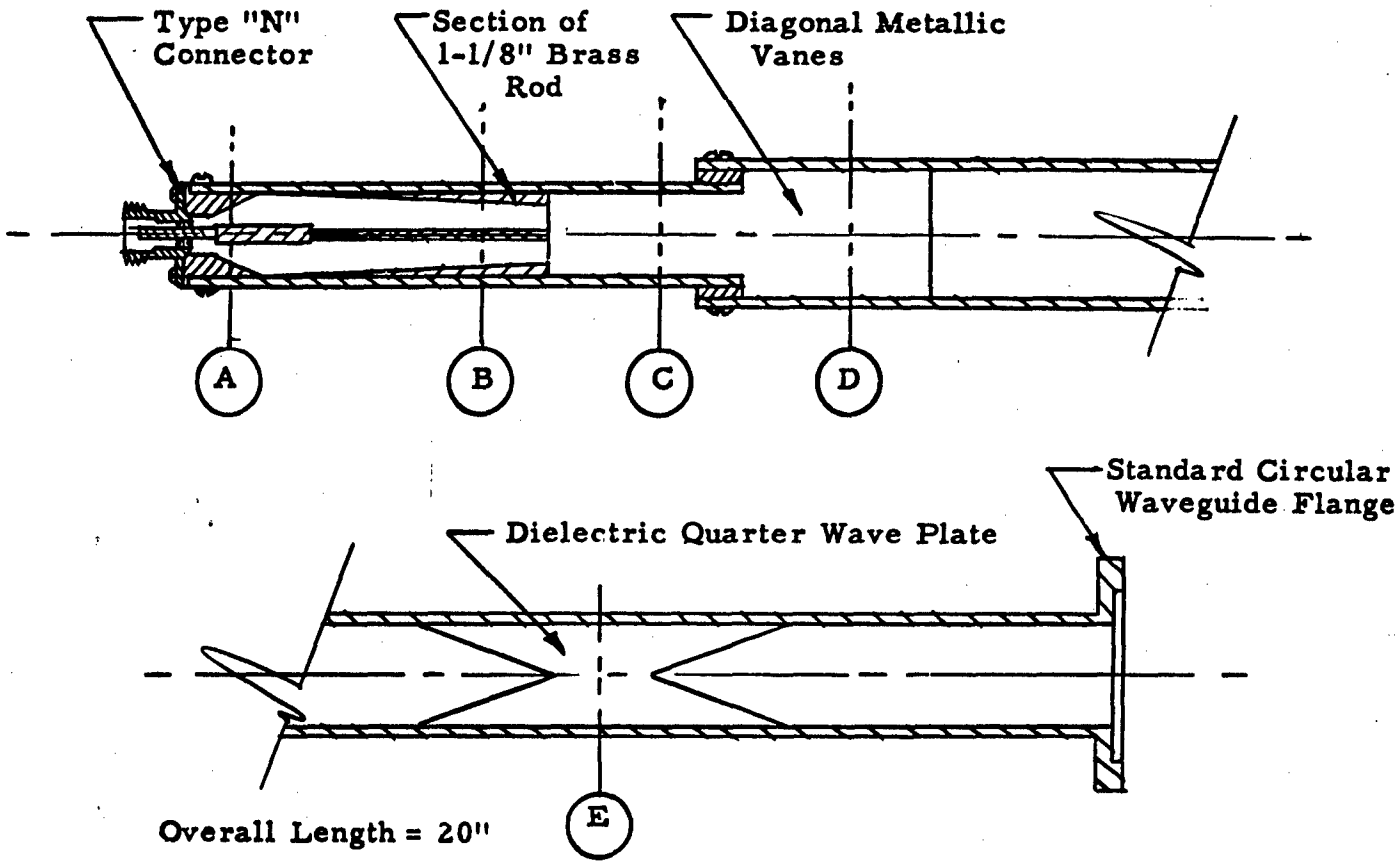

Figure 10. Mode Transducer.

The input to the transducer is from a TEM mode in a coaxial line. Because of the symmetry of the input section, a TE_{01} mode is excited in the top "X" band waveguide 180° out of phase with the TE_{01} mode excited in the bottom waveguide. Cylindrical bevels then shape the field lines in the two waveguides until they combine to have approximately the shape of the TE_{11} mode in a square waveguide. The wall separating the two waveguides is then ended, and, by Huygen's principle[2], the shape of the field lines dictates that mainly the TE_{11} mode shall be excited in the resulting square waveguide. To insure this result, diagonal metallic vanes are placed in the guide so that the composite sections of the TE_{11} modes are actually the only non-cut off modes in the four triangular waveguides formed by the diagonal vanes. Since the TE_{11} mode in a square waveguide has a field line configuration very close to the shape of the field lines of the TE_{21} mode in a circular guide, again by Huygen's principle, the only mode excited in the circular waveguide when the square guide is changed to circular guide should be the TE_{21} mode. The diagonal metallic vanes are continued into the circular guide two inches to suppress any other modes. After the TE_{21} mode is obtained, the dielectric quarter wave plate is inserted. Since the maximum concentration of the TE_{21} mode forms a cross in the guide, two perpendicular plates must be inserted at 22-1/2° from a maximum of the total field (See figure 11).

Once it has been determined that the transducer is providing the desired rotating TE_{21} mode, the only measurements necessary are the scattering coefficients measurements. The scattering coefficients describe the efficiency of the transducer as well as how good a match

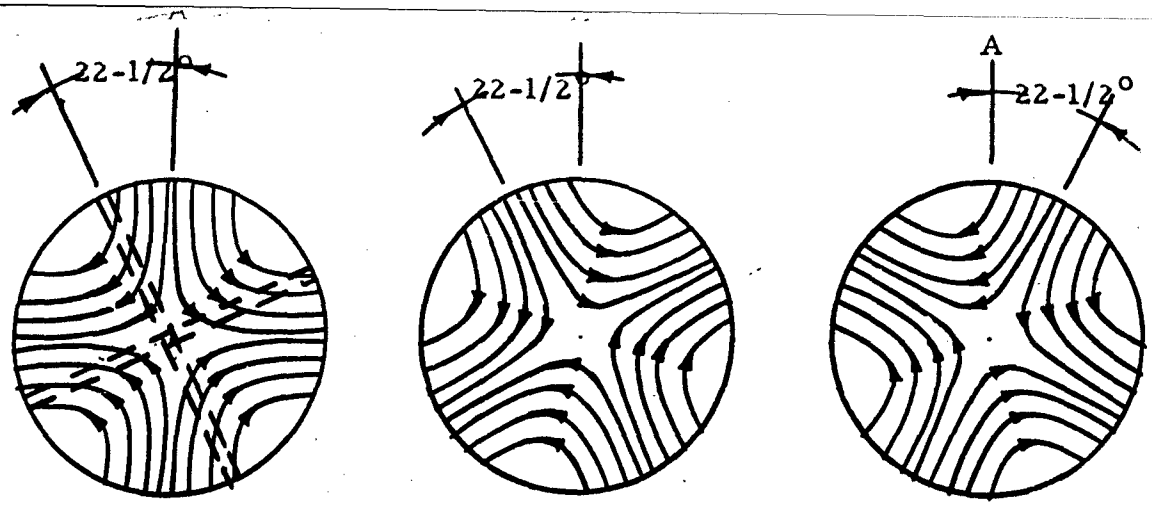

Total Field and Position of Quarter Wave Plates

Orthogonal Components

Figure 11. Orientation of Quarter Wave Plates

it presents looking in from the ends. The method that will be used to measure the scattering coefficients is the method of Deschamps[3], which is based on the geometric properties of bilinear transformations of Smith Chart plots. His method is especially applicable to this transducer because it does not require the same mode at the input and output terminals of the transducer, and it allows for a lossy network or an imperfect shorting plane. However, it has not been possible to carry out the scattering coefficient measurements yet because the transducer is not presenting only one mode at its output terminals. One indication that only one mode is present is given when, with the quarter wave plate in place, measurements of the magnitude of the field around the azimuth of the waveguide are the same. The best that this condition could be approached so far was an axial ratio of 4:1. When the quarter wave plate is not in place and the shorting plane is positioned so that the largest signal is received by probe "B"

(see figure 12.) the azimuthal variation of the radial component of the electric field seems to be very definitely that of a pure TE_{21} linearly polarized mode; while when the shorting plane is positioned so that a minimum signal is received by probe "B" or with a matched load the measurements indicate the presence of a good percentage of undesired modes.

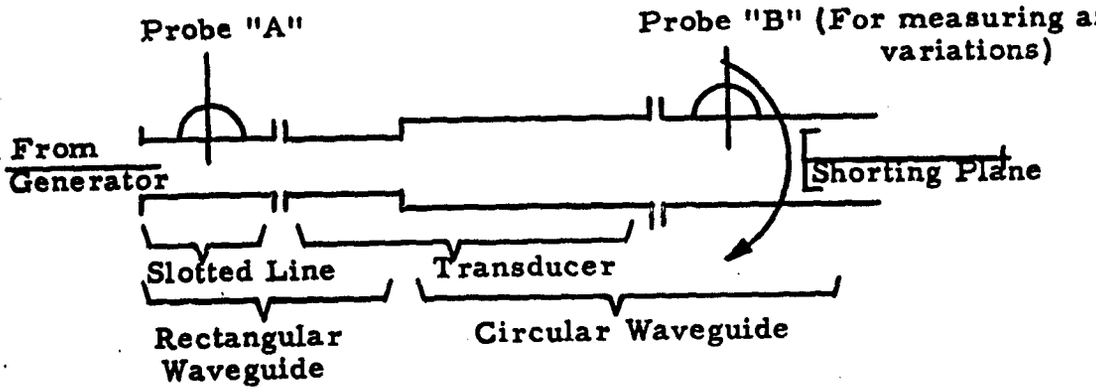

Experimental Setup

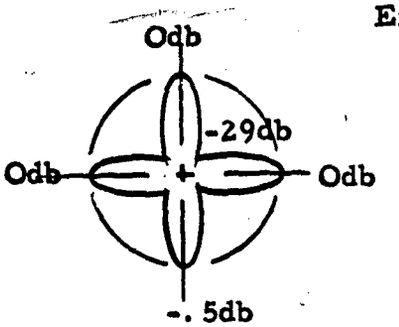

Azimuthal variations measured when shorting plane position gives maximum signal at probe "B".

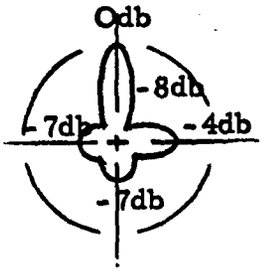

Azimuthal variations measured when using a matched load termination.

Figure 12. Measuring Techniques and Data

The main clue as to the reason for the unsatisfactory operation of the transducer is the fact that with the shorting plane in position the VSWR measured at the input by probe "A" ranges between 4:1 and

1.1:1, which is much too low for a supposedly lossless transducer. Presently, the VSWR is being measured by placing shorting planes at various points inside the transducer in order to isolate the location of the introduction of losses.

Several interesting theoretical results have been obtained from the investigations of the above transducer.

(1) Nonexistence of Circularly Polarized Waves in Enclosed Waveguides.

It is possible to prove the impossiblity of the existence of a circularly polarized wave in a cylindrical waveguide with an enclosed cross-section of arbitrary shape as follows:

If a wave is circularly polarized and is propagating in the $\hat{z}$ direction, then, by definition, at every point:

$$E_x e^{j\omega t} = E_y e^{j(\omega t \pm \pi/2)} \tag{4}$$

$$\text{or:} \quad E_x = \pm j E_y \tag{5}$$

$$\text{For TE modes:} \quad \bar{E}_{\text{transverse}} = -\hat{z} \times \nabla f_{TE} \tag{6}$$

$$\text{and for TM modes:} \quad E_{\text{transverse}} = \nabla_t \left(\frac{\partial f_{TM}}{\partial E} \right) = -\gamma_z \nabla_t f_{TM} \tag{7}$$

where f_{TE} and f_{TM} are the TE and TM Hertz potential functions, respectively. Then by equation (5):

$$\frac{\partial f}{\partial x} = \pm j \frac{\partial f}{\partial y} \tag{8}$$

Differentiating with respect to x:

$$\frac{\partial^2 f}{\partial x^2} \mp j \frac{\partial^2 f}{\partial y \partial x} = 0 \tag{9}$$

But since $\frac{\partial f}{\partial x} = \pm j \frac{\partial f}{\partial y}$, (9) becomes:

$$\frac{\partial^2 f}{\partial x^2} \mp j(\pm j) \frac{\partial^2 f}{\partial y^2} = \frac{\partial^2 f}{\partial x^2} + \frac{\partial^2 f}{\partial y^2} = 0 \tag{10}$$

Hence f obeys Laplace's equation and is a harmonic function.

Since $E_{tangential} = 0$ at the walls of a waveguide, then by equation (5):

$$E_x = \pm j E_y = 0 \qquad \text{at walls} \tag{11}$$

This means, by (6) and (7):

$$\frac{\partial f}{\partial x} = \pm j \frac{\partial f}{\partial y} = 0 \tag{12}$$

along the walls of the waveguide. Hence f must be a constant around the periphery of the waveguide. But it is known that a harmonic function that is constant on a closed boundary and whose normal derivative vanishes at the boundary must be constant throughout the enclosed region. Hence by (6) and (7):

$$E_x = \pm j E_y = 0 \tag{13}$$

throughout the waveguide.

It is thus shown that the assumption of a circularly polarized wave in a waveguide of closed cross-section implies zero fields within the guide.

(2) Fields in a Lossless Cavity

In a lossless cavity with electric current sources only, Maxwell's equations and the boundary conditions may be written:

$$\begin{aligned} \nabla \times \bar{E}_d &= - j\omega\mu \bar{H}_d \\ \nabla \times \bar{H}_d &= j\omega\epsilon \bar{E}_d + \bar{J}_d \\ \hat{n} \times \bar{E}_d &= 0 \qquad \text{on the walls of the cavity.} \end{aligned} \tag{14}$$

$\hat{n}$ is a unit vector perpendicular to the walls of the cavity. Now, if the conjugate of equations (14) is taken, we find:

$$\nabla \times \bar{E}_d^* = j\omega\mu \bar{H}_d^*$$

$$\nabla \times \bar{H}_d^* = -j\omega\epsilon \bar{E}_d^* + \bar{J}_d^* \qquad (15)$$

$$\hat{n} \times \bar{E}_d^* = 0 \quad \text{on the walls of the cavity.}$$

If we set a field $\underline{f}$ equal to the following quantities: $\bar{E}_f = -\bar{E}_d^*$; $\bar{H}_f = \bar{H}_d^*$ we have from equations (15):

$$\nabla \times \bar{E}_f = -j\omega\mu \bar{H}_f$$

$$\nabla \times \bar{H}_f = j\omega\epsilon \bar{E}_f + \bar{J}_d^* \qquad (16)$$

$$n \times \bar{E}_f = 0 \quad \text{on the walls of the cavity.}$$

Thus by comparing equation (16) to (14) we see that $\bar{E}_f$ and $\bar{H}_f$ are the fields of the source $\bar{J}_d$ in the same cavity. Now if $\bar{J}_d$ is real, $\bar{J}_d = \bar{J}_d^*$ and by the uniqueness theorem $\underline{f}$ is the same field as $\underline{d}$. Hence:

$$\bar{E}_d = \bar{E}_f = -\bar{E}_d^*$$

$$\bar{H}_d = \bar{H}_f = \bar{H}_d^* \qquad (17)$$

Thus for a real source $\bar{J}_d$ in a lossless cavity, the magnetic field is pure real everywhere while the electric field is pure imaginary everywhere.

Now if we choose field $\underline{g}$ such that $\bar{E}_g = \bar{E}_d^*$; $\bar{H}_g = -\bar{H}_d^*$ then, from equations (15)

$$\nabla \times \bar{E}_g = -j\omega\mu \bar{H}_g$$

$$\nabla \times \bar{H}_g = j\mu\epsilon \bar{E}_g - \bar{J}_d^* \qquad (18)$$

$$n \times \bar{E}_g = 0 \quad \text{on the walls of the cavity.}$$

Thus by comparing equations (14) to (18) we see that if we assume J_d is pure imaginary, then $\overline{J}_d = -\overline{J}_d^*$ and $\overline{E}_g$ and $\overline{H}_g$ are also the fields of $\overline{J}_d$ in the lossless cavity and by the uniqueness theorem g is the same field as d hence:

$$\overline{E}_d = \overline{E}_g = \overline{E}_d^*$$

$$\overline{H}_d = \overline{H}_g = -\overline{H}_d^* \tag{19}$$

Thus for a pure imaginary source $\overline{J}_d$ in a lossless cavity the electric field is pure real everywhere, while the magnetic field is pure imaginary everywhere.

Equations (17) and (19) help to point out some interesting predictions. First, we can know, if we assume the transducer lossless, that it is impossible to have a rotating mode present in the guide with the shorting plane present at one end. The reason this is so, is because the coaxial line feed supports a TEM mode. Since the transverse magnetic field in the coax is all in phase at one cross-section in the coaxial guide, we may replace it by an electric current Huygen's source that is pure real backed by a magnetic conducting plane. Since we have now a real electric current source in a lossless cavity (all the above relations still hold if we add n x H = 0 to the boundary conditions), we know by equations (17) that the magnetic field is pure real everywhere thus ruling out the possibility of a rotating mode in the transducer when terminated by a shorting plane.

Another result that can be shown is that if we have a rotating mode current as the source present in the lossless cavity it is possible to have rotating fields present in the cavity. This can be shown by an example of two TE_{11} modes in a right circular cylinder shorted at each end. The rotating source current can be broken into two components, one at right angles to the other spatially and lagging it by 90° in time. Hence one source is pure real and gives rise to a pure imaginary TE_{11} electric field by equations (17) while the other source is pure imaginary and gives rise to a pure real TE_{11} electric field

by equations (19) and at right angles to the first field. Since the two fields are orthogonal, we know then that the total field will remain the sum of the two component fields. Because of the 90^{o} spatial and 90^{o} time orientation of the two fields, the resulting field will be a rotating field.

It is also possible to show that a rotating mode can exist in a lossless cavity with no sources. If $\overline{J}_d = 0$ in equations (14) - (19), we see that both electric field types $\overline{E}_f$ and $\overline{E}_g$ are possible; i.e., the electric field can be both real or imaginary. Now in a lossless cavity with no sources, the field present is determined by the boundary conditions and the initial conditions. Since we have shown by equations (14) - (19) that we can satisfy the boundary conditions with a rotating mode, it merely remains to show that we can set up the necessary initial conditions. This can be done easily, as is shown in the following example: Suppose a rotating source is placed at the left end of a lossless cavity that is several wavelengths long. Then slide a shorting plane into a point in the cavity standing wave where the electric field is zero. The region to the right of the shorting plane will thus be a lossless cavity with no sources whose initial condition was the presence of a rotating mode.

In order to present a more complete picture of the rotating mode in the lossless cavity, the Poynting vector is calculated for the TE_{11} mode and shown to be zero as follows:

$\overline{E}$ = total electric field of the rotating TE_{11} mode

$\overline{H}_T$ = total transverse magnetic field of the rotating TE_{11} mode

Let: $\overline{E}_1$ = real part of $\overline{E}$

and $\overline{E}_2$ = imaginary part of $\overline{E}$

Then by equations (14) - (19):

$$\overline{E}_1 = \overline{E}_1^* \qquad \overline{E}_2 = -\overline{E}_2^*$$

and

$$\overline{H}_1 = -\overline{H}_1^* \qquad \overline{H}_2 = \overline{H}_2^*$$

Since the field is a pure rotating TE_{11} mode, the 1 and 2 modes are displaced azimuthally by 90°. Then by the standard form of the linearly polarized TE_{11} fields in a cavity: (where β is the propagation constant in the $\hat{z}$ direction).

$$\bar{E}_1 = \hat{\rho}\, e_\rho(\rho, z) \sin\phi + \hat{\phi}\, e_\phi(\rho, z) \cos\phi \tag{20}$$

where $e_\rho(\rho, z)$ and $e_\phi(\rho, z)$ are pure real functions. And:

$$\bar{H}_{1T} = [\hat{\rho} e_\phi(\rho, z) \cos\phi - \hat{\phi}\, e_\rho(\rho, z) \sin\phi] \frac{\beta \cot \beta z}{j\omega\mu} \tag{21}$$

Whereas:

$$\bar{E}_2 = j[\hat{\rho}\, e_\rho(\rho, z) \cos\phi - \hat{\phi}\, e_\phi(\rho, z) \sin\phi] \tag{22}$$

and

$$\bar{H}_{2T} = [\hat{\rho} e_\phi(\rho, z) \sin\phi + \hat{\phi} e_\rho(\rho, z) \cos\phi\ ] \frac{-\beta \cot \beta_z}{\omega\mu} \tag{23}$$

Therefore:

$$\bar{E} = \bar{E}_1 + \bar{E}_2 = \hat{\rho}\, e_\rho(\rho, z)\, [\sin\phi + j\cos\phi] + \hat{\phi}\, e_\phi(\rho, z)[\cos\phi - j\sin\phi] \tag{24}$$

or $$\bar{E} = j\hat{\rho}\, e_\rho(\rho, z)\, e^{j\phi} + \hat{\phi}\, e_\phi(\rho, z)\, e^{-j\phi} \tag{25}$$

and $$\bar{H}_T = \bar{H}_{1T} + \bar{H}_{2T} = \frac{\beta \cot \beta_z}{\omega\mu} \{\hat{\rho}\, e_\phi(\rho, z)\, [-j\cos\phi - \sin\phi] + \hat{\phi} e_\rho(\rho, z)[j\sin\phi - \cos\phi]\} \tag{26}$$

or $$\bar{H}_T = \frac{\beta \cot \beta_z}{\omega\mu} [\hat{\rho}\, e_\phi(\rho, z)\, e^{-j\phi}(-j) - \hat{\phi}\, e_\rho(\rho, z)(-e^{-j\phi}) \tag{27}$$

and $$\bar{H}_T^* = \frac{\beta \cot \beta_z}{\omega\mu} [\hat{\rho}\, e_\phi(\rho, z)\, (je^{j\phi}) + \hat{\phi}\, e_\rho(\rho, z)\, (-e^{j\phi})] \tag{28}$$

The average Poynting vector may now be calculated:

$$\bar{E} \times \bar{H}_T^* = E_\rho H_\phi^* - E_\phi H_\rho^* \tag{29}$$

$$E \times \bar{H}_T^* = \frac{-\beta \cot \beta_z}{\omega \mu} \left[[e_\rho(\rho, z)]^2 + [e_\phi(\rho, z)]^2 \right] j \tag{30}$$

Therefore; $\frac{1}{2} \mathrm{Re}(\bar{E} \times \bar{H}^*) = 0$ as required for fields in a lossless cavity.

2. Pattern Recorder

In order to provide more accurate recording of antenna patterns than what was previously available with our equipment, a somewhat novel recording apparatus was constructed. Its principle of operation is as follows. The test antenna is mounted on a turn table which rotates at a constant angular velocity. This antenna broadcasts to a fixed antenna whose output is fed to an indicator through an adjustable attenuator and an amplifier. The operator observes the indicator and continuously adjusts the attenuator to keep the indication constant. The precision rotary waveguide attenuator is ganged to two helipot voltage dividers in series that are externally loaded with resistors, so that the attenuation is translated directly into voltage. This voltage is fed to a time base voltage recorder. With the antenna under test rotating at the rate of one revolution every five minutes, it is possible to maintain an accuracy of one db over a dynamic range of 40 db.

OVERALL CONCLUSIONS AND RECOMMENDATIONS

The conclusions derived from much of this work are summarized in the abstracts of the reports quoted in the "Factual Data" section of this reportpages 2-8. The conclusions derived from the work not covered in these reports, are described in the next paragraph. It is recommended that the remarkable predictions of the theoretical solution for the multielement plane spiral antenna, especially the inward current wave at large distances caused by exciting the spiral in the "unnatural" sense of rotation, be checked experimentally. The unusual experimental results due to higher order types of excitation for multi-

element spiral antennas described in Sussman's report should be followed up. The theory of periodic antennas should be developed further and extended to logarithmically periodic structures, and the theory of conical structures, which is at present close to solution should be pursued.

Theoretically, the excitation of the multiarm planar spiral antenna by a waveguide normal to the center is attractive because it enables the use of the antenna at "X" band frequencies to facilitate pattern measurements. It also allows a greater number of arms to be used on the antenna and thereby approach the ideal anisotropic antenna. However, it was found that difficulties arise when attempting to feed the antenna with the waveguide. First, the waveguide must excite the antenna over a region which does not include the active radiating region. This was avoided by using a tapered dielectrically loaded waveguide. The next problem was the difficulty in obtaining effective coupling to the antenna when connecting all the antenna arms to the inner conductor of the coaxial feed waveguide. Also, for the $e^{\pm j\phi}$ mode, the feed waveguide is found to lay in the maximum of the antenna pattern, thereby representing a major disturbance to the field. Theoretically, the $e^{\pm jn\phi}$ modes, where $n > 1$, have a null in their patterns at the location of the feed waveguide. It is therefore recommended that further attempts to be made to excite especially the $e^{\pm j2\phi}$ mode on the antenna by using a sectionalized outer conductor on the waveguide placed between the dielectrically loaded tapered waveguide and the antenna. Each section of this outer conductor should be connected to a corresponding arm of the antenna, so as to obtain better coupling to the antenna.

The investigation of a helix in a circular waveguide has shown that it does not present much possibility as a method of providing rotating modes. However, it is recommended that further investigations be made along this line for two reasons. First, the multifilar helix might be used as a device for converting a linearly polarized TE_{11} mode in a circular waveguide to a rotating TEM mode in a multiconductor cable (i.e., like a polyphase cable) of small dimensions. Each conductor of this cable could then be connected to an arm of the antenna to provide

a good coupling to the antenna. Also, the complicated dispersion relationships arrived at could be set up for solution by a computer, thus showing whether it contains any stop bands for any of the modes. Stop bands in an enclosed guide would be an enlightening phenomena to help explain how the stop bands of certain modes on periodic structures in free space account for the major portion of radiation from the structures.

Since the TE_{21} mode transducer is considered to be theoretically correct in design, more effort should be placed in finding the flaw in the construction which prevents it from providing a pure TE_{21} mode, independent of the position of the terminating shorting plane. The particular method most likely to find this flaw is that of placing a shorting plane at progressive stages along the transducer until the VSWR at the input goes from a large value to a small value. Since the transducer supposedly is nearly lossless, it should present a large VSWR at its input when shorted anywhere inside; however, with a shorting plane at the output of the transducer, an excessively low VSWR is measured at the input, thus indicating that too much loss is being introduced at some point in the transducer. The TE_{21} mode transducer is designed to provide the $e^{j2\phi}$ excitation mentioned above.

REFERENCES

1. V. H. Rumsey, "Study of Frequency Independent Antennas, Report No. 2," Electronics Research Laboratory Second Quarterly Progress Report, 1 August 1960 - 31 October 1960, University of California, Berkeley, California.
2. V. H. Rumsey, "Some New Forms of Huygen's Principle," I. R. E. P. G. A. P. v AP-7, pp. 103-116, Dec., 1959.
3. G. A. Deschamps, "Determination of Reflection Coefficients and Insertion Loss of a Waveguide Junction," J. A. P., v 24, n 8, Aug. 1953.
4. V. H. Rumsey, "A Complete Orthogonal Set of Solutions for Maxwell's Equations with Applications to Anisotropic Sheets," Electronics Research Laboratory, Series 60, Issue No. 287 June 15, 1960.
5. V. H. Rumsey, "A New Way of Solving Maxwell's Equations," Electronics Research Laboratory, Series 60, Issue No. 335, December 19, 1960

6. B. R-S. Cheo, "A Solution to the Equiangular Spiral Antenna Problem," Electronics Research Laboratory, Series 60, Issue No. 324

7. B. Cheo, V. H. Rumsey, and W. J. Welch, "A Solution to the Frequency-Independent Antenna Problem," Electronics Research Laboratory Series 60, Issue No. 372, June 14, 1961

8. G. Borgiotti and V. H. Rumsey, "Propagation over a Sheet of Sinusoidal Waves with Application to Frequency Independent Antennas," Electronics Research Laboratory, to be published.

9. J. Siambis, "Polarization Properties of Plane Equiangular Spiral Antennas," Electronics Research Laboratory, to be published.

10. R. Sussman, "The Equiangular Plane Spiral Antenna", Electronics Research Laboratory, to be published.

11. N. Barbarno, "Phase Distributions of Spiral Antennas," Electronics Research Laboratory, Series 60, Issue No. 266

12. R. Sussman, "The Equiangular Plane Spiral Antenna," Electronics Research Laboratory, to be published

AD_____ Accession No. _____

Electronics Research Laboratory, University of California, Berkeley 4, California.
FREQUENCY-INDEPENDENT ANTENNAS — V. H. Rumsey, W. J. Welch, G. Borgiotti, M. J. Gans, R. Sussman. Final Progress Report No. 4, 1 February 1961 to 30 April 1961. pp + ill. Contract DA 36-039 SC-84923. Unclassified Report.

During the past year solutions of Maxwell's equations have been discovered which explain the theory of frequency independent antennas. The effect of curvature on the current distribution is strikingly demonstrated but the most remarkable feature is the incoming current wave at large distances, when the angular phase velocity of the excitation is in the direction of decreasing radius along an equiangular spiral. Solutions for periodic antennas have also been obtained and extensive computations are being made.

Unclassified

1. Frequency Independent Antennas.
2. Contract DA 36-039 SC-84923

AD_____ Accession No. _____

Electronics Research Laboratory, University of California, Berkeley 4, California.
FREQUENCY-INDEPENDENT ANTENNAS — V. H. Rumsey, W. J. Welch, G. Borgiotti, M. J. Gans, R. Sussman. Final Progress Report No. 4, 1 February 1961 to 30 April 1961. pp + ill. Contract DA 36-039 SC-84923. Unclassified Report.

During the past year solutions of Maxwell's equations have been discovered which explain the theory of frequency independent antennas. The effect of curvature on the current distribution is strikingly demonstrated but the most remarkable feature is the incoming current wave at large distances, when the angular phase velocity of the excitation is in the direction of decreasing radius along an equiangular spiral. Solutions for periodic antennas have also been obtained and extensive computations are being made.

Unclassified

1. Frequency Independent Antennas.
2. Contract DA 36-039 SC-84923

AD_____ Accession No. _____

Electronics Research Laboratory, University of California, Berkeley 4, California.
FREQUENCY-INDEPENDENT ANTENNAS — V. H. Rumsey, W. J. Welch, G. Borgiotti, M. J. Gans, R. Sussman. Final Progress Report No. 4, 1 February 1961 to 30 April 1961. pp + ill. Contract DA 36-039 SC-84923. Unclassified Report.

During the past year solutions of Maxwell's equations have been discovered which explain the theory of frequency independent antennas. The effect of curvature on the current distribution is strikingly demonstrated but the most remarkable feature is the incoming current wave at large distances, when the angular phase velocity of the excitation is in the direction of decreasing radius along an equiangular spiral. Solutions for periodic antennas have also been obtained and extensive computations are being made.

Unclassified

1. Frequency Independent Antennas.
2. Contract DA 36-039 SC-84923

AD_____ Accession No. _____

Electronics Research Laboratory, University of California, Berkeley 4, California.
FREQUENCY-INDEPENDENT ANTENNAS — V. H. Rumsey, W. J. Welch, G. Borgiotti, M. J. Gans, R. Sussman. Final Progress Report No. 4, 1 February 1961 to 30 April 1961. pp + ill. Contract DA 36-039 SC-84923. Unclassified Report.

During the past year solutions of Maxwell's equations have been discovered which explain the theory of frequency independent antennas. The effect of curvature on the current distribution is strikingly demonstrated but the most remarkable feature is the incoming current wave at large distances, when the angular phase velocity of the excitation is in the direction of decreasing radius along an equiangular spiral. Solutions for periodic antennas have also been obtained and extensive computations are being made.

Unclassified

1. Frequency Independent Antennas.
2. Contract DA 36-039 SC-84923

DISTRIBUTION LIST	COPY NUMBER
Chief, Advanced Development Branch Radar Division, Surveillance Dept. USASRDL, Evans Area, Belmar, N.J.	1, 2
Commanding Officer U.S. Army Signal Research & Development Lab. Fort Monmouth, N.J. ATTN: SIGRA/DR	3
SIGRA/SL-ADTE	4
SIGRA/SL-SC	5, 6
SIGRA/SL-LNF	7, 8, 9
SIGRA/SL-LNS	10
SIGRA/SL-TNR	11, 12, 13
Commanding Officer U.S. Army Signal Research and Development Lab. Fort Monmouth, N.J. ATTN: Ch, Technical Staff, Radar Division thence to File Unit No. 3 (for File)	14
Chief Signal Officer Department of the Army Washington 25, D.C. ATTN: SIGRD	15
SIGRD-9	16
Commanding Officer Diamond Ordnance Fuze Laboratory Connecticut Ave. & Van Ness Street Washington 25 D.C.	17
Sylvania Electronics System Reconnaissance Systems Lab P.O. Box 188 Mountain View, California	18
Commanding Officer U.S. Army Signal Missile Support Agency White Sands Missile Range, New Mexico ATTN: ORDBS-IRM-RID-M	19
Commander, U.S. Air Force Security Service San Antonio, Texas ATTN: MFE	20
Chief, Intelligence Agency 2430 "E" Street, N.W. Washington 25, D.C. ATTN: Liaison Div., CCR-REF: Control No. LD 5701.1	21
Major R.J. Corry Canadian Army Liaison Officer OCSIGO, Rm. 2D244, The Pentagon Washington 25, D.C.	22
Defense Research Member Canadian Joint Staff 2450 Massachusetts Avenue, N.W. Washington 8, D.C.	23
Chief, Security Division USASRDL, ATTN: Mr. E. McDermott (for Transmittal to) National Research Council Radio & Electrical Engineering Div. Ottowa, Ontario, Canada	24
NASA, Goddard Space Flight Center Code 523 Greenbelt, Maryland Attn: Mr. Paul A. Lantz	25
Space Technology Labs, Inc. Box 95001 Los Angeles 45, California ATTN: Dr. R.C. Hansen	26
Chief, U.S. Army Security Agency Arlington Hall Station Arlington 12, Virginia ATTN: OCS of Dev	27
Deputy President U.S. Army Security Agency Board Arlington Hall Station Arlington 12, Virginia	28
Commanding Officer U.S. Army Signal Electronic Research Unit P.O. Box 205 Mountain View, California	29
Commanding General U.S. Army Electronic Proving Ground Fort Huachua, Arizona	30
Director U.S. Naval Research Laboratory Code 2027 Washington 25, D.C.	31
Commanding Officer & Director U.S. Navy Electronics Laboratory San Diego 52, California	32
Commander Wright Air Development Division Wright-Patterson Air Force Base, Ohio ATTN: WCOSI-3	33
WCLRS-6, Mr. W.J. Portune	34
Commander Air Force Cambridge Research Laboratories CROOTR, L.G. Hanscom Field Bedford, Massachusetts	35
Commander Armed Services Technical Information Agency Arlington Hall Station Arlington 12, Virginia	36, 37, 38, 39 40, 41, 42
Chief, Bureau of Aeronautics Department of the Army Washington 25, D.C. ATTN: Code AV-4421	43
Director U.S. Navy Underwater Sound Laboratory New London, Connecticut ATTN: Code 1310, Mr. R.W. Turner	44
Commander New York Naval Shipyard Brooklyn 1, New York ATTN: Code 932, Mr. D. First, Material Laboratory	45
Director, Ballistic Research Laboratories Aberdeen Proving Ground Aberdeen, Maryland ATTN: Ballistic Measurement Laboratory	46
National Security Agency 3801 Nebraska Avenue, N.W. Washington 25, D.C. ATTN: RADE-1	47
Commander, Rome Air Development Center Griffiss Air Force Base Rome, New York ATTN: RCSST-3	48
NUMNSS	49
RCOIL-2	50

This contract is supervised by Radar Division, Surveillance Dept., USASRDL, Belmar, N.J. For further information, contact Chief, Advanced Development Branch, Radar Division, Surveillance Dept., USASRDL, Belmar, N.J. Telephone 59 - 61655. Contracting Officer's Technical Representatives: Messrs. J.C. Ackerman and V.L. Friedrich, Radar Division, Surveillance, Dept., USASRDL, Belmar, N.J.